Izet Horman, Seid Hajdarević, Sandra Martinović, Nikola Vukas[1]

Numerical Analysis of Stress and Strain in a Wooden Chair

Numerička analiza naprezanja i deformacija u drvenoj stolici

ABSTRACT • *This paper presents numerical analysis of stress and strain conditions of a three-dimensional furniture skeleton construction and its joints. The finite volume method is used in the calculation. Orthotropy of the wood material is accounted for by approximating it with an isotropic material whose elastic modulus and Poisson's ratio are calculated by employing the least-square method. The displacement of the edge point for the loaded joint was also determined experimentally. The agreement of results of the calculation and experimental data can be considered satisfactory. The numerical results presented in this paper also provided an opportunity for identification of the region with the largest load and strain in the complex chair skeleton construction, which is one of the most complex pieces of furniture.*

Key words: corner joint, chair, displacement, stress, wood, numerical analysis

SAŽETAK • *U radu je prikazana numerička analiza naprezanja i deformacija prostorne okvirne konstrukcije namještaja i spojeva koji se u njoj pojavljuju. Za proračun je korištena metoda konačnih volumena. Zanemarena je ortotropija, a modul elastičnosti i Poissonov omjer za simulirani izotropni materijal aproksimirani su metodom najmanjih kvadrata. Za opterećeni kutnik pomak rubne točke i eksperimentalno je određen. Rezultati proračuna zadovoljavajuće se slažu s eksperimentalnim podacima, pa se predloženi numerički algoritam može primijeniti za analizu krutosti i čvrstoće spojeva. Numerički rezultati dani u ovom radu omogućili su identificiranje mjesta najvećeg opterećenja i deformacije u složenoj okvirnoj konstrukciji stolice kao jednome od najsloženijih komada namještaja.*

Ključne riječi: kutni spoj, stolica, pomak, naprezanje, drvo, numerička analiza

1 INTRODUCTION
1. UVOD

Development of new products in the wood industry in the past was mostly based on empiric information. The data about construction properties were usually obtained by testing prototypes of the final product. The development of computer technology and numerical methods have made the research much easier and enabled obtaining information of what is happening inside a loaded chair already at the design stage. Their use in the industry saves the time for the product development and improves its quality. For example, at the design stage of some pieces of furniture, their complex skeleton construction is subjected to stress and strain analysis. That allows them to satisfy all the functional demands

[1] Authors are associated professor, senior assistant, assistant and assistant professor at Faculty of Engineering, University of Sarajevo, Sarajevo, Bosnia and Herzegovina.
[1] Autori su izvanredni profesor, viši asistent, asistentica i docent na Mašinskom fakultetu Sveučilišta u Sarajevu, Sarajevo, Bosna i Hercegovina.

(comfort), aesthetic demands, but also the strength and stiffness both by their shape and their dimensions. To achieve that, it is necessary to carry out a numerical simulation of the stress of a complex construction.

The study of the literature has established that the most frequent method applied in calculating the stress and strain in solid bodies was finite element method (Nicholls and Crisan, 2002; Smardzewski and Prekrat, 2002; Olsson P. and Olsson K., 2003; Pousette 2003; Smardzewski and Papuga, 2004; Pousette, 2006) and more recently the finite volume method (Demirdžić and Martinović, 1993; Demirdžić and Muzaferija, 1995; Demirdžić *et al.*, 2000; Martinović *et al.*, 2001; Horman *et al.*, 2008; Horman *et al.*, 2009). Calculations in this study are performed by employing the software package COMET (ICCM 2001) which applies the finite volume method for analysing stress in elastic, isotropic bodies of arbitrary shape. As wood is an orthotropic material, it is simulated by isotropic one and the mechanical properties are approximated by the least-square method (Heyden, 2000).

This paper first analyses the stress-strain state in a corner joint, and then in a complex, loaded chair skeleton, because the quality and durability of a complex skeleton construction primarily depends on the quality of its joints. The regions exposed to the largest strains and stresses are identified. The paper also presents the experimental determination of displacement of the targeted corner joint point, which serves to verify the numerical results.

2 MATHEMATICAL MODEL
2. MATEMATIČKI MODEL

2.1 Basic equations and constitutive relations
2.1. Osnovne jednadžbe i konstitutivne relacije

The equation of momentum balance, expressed in the Cartesian tensor notation (Slattery, 1981)

$$\int_S \sigma_{ij} n_j dS + \int_V f_i dV = 0 \qquad (1)$$

and of the constitutive relation for the elastic material

$$\sigma_{ij} = C_{ijkl}\varepsilon_{kl} = \frac{1}{2}C_{ijkl}\left(\frac{\partial u_k}{\partial x_l} + \frac{\partial u_l}{\partial x_k}\right) \qquad (2)$$

describe the stress and strain of a loaded solid body in the static equilibrium.

Equation (2) for the elastic, orthotropic material may be expressed in the following matrix form (Bodig and Jayne, 1993).

$$
\begin{bmatrix} \sigma_{11} \\ \sigma_{22} \\ \sigma_{33} \\ \sigma_{12} \\ \sigma_{23} \\ \sigma_{31} \end{bmatrix} =
\begin{bmatrix}
A_{11} & A_{12} & A_{13} & 0 & 0 & 0 \\
A_{21} & A_{22} & A_{23} & 0 & 0 & 0 \\
A_{31} & A_{32} & A_{33} & 0 & 0 & 0 \\
0 & 0 & 0 & A_{44} & 0 & 0 \\
0 & 0 & 0 & 0 & A_{55} & 0 \\
0 & 0 & 0 & 0 & 0 & A_{66}
\end{bmatrix}
\begin{bmatrix} \varepsilon_{11} \\ \varepsilon_{22} \\ \varepsilon_{33} \\ \varepsilon_{12} \\ \varepsilon_{23} \\ \varepsilon_{31} \end{bmatrix} \qquad (3)
$$

In the equations above, x_j are the Cartesian spatial coordinates, V is the volume of the solution domain bounded by the surface S, σ_{ij} is the stress tensor, n_j is the out warded unit normal to the surface S, f_i the volume force, C_{ijkl} the elastic constant tensor components, ε_{kl} the

strain tensor, and u_k the point displacement. Twelve non-zero orthotropic elastic constants A_{ij} are related to the Young's modulus E_i, the Poisson's ratio v_{ij} and the shear modulus G_{ij} by the following relations:

$$A_{11} = \frac{E_1}{C}(1 - v_{23}v_{32}),\ A_{22} = \frac{E_2}{C}(1 - v_{31}v_{13}),$$

$$A_{33} = \frac{E_3}{C}(1 - v_{12}v_{21}),\ A_{12} = A_{21} = \frac{E_1}{C}(v_{21} + v_{31}v_{23}),$$

$$A_{13} = A_{31} = \frac{E_1}{C}(v_{31} + v_{21}v_{32}),$$

$$A_{23} = A_{32} = \frac{E_2}{C}(v_{32} + v_{12}v_{31}) \qquad (4)$$

$$A_{44}=2G_{12},\ A_{55}=2G_{23},\ A_{66}=2G_{31}$$

$$C=1 - v_{12}v_{21} - v_{23}v_{32} - v_{31}v_{13} - v_{12}v_{23}v_{31} - v_{21}v_{32}v_{13},$$

where

$$E_1v_{21}=E_2v_{12},\ E_1v_{31}=E_3v_{13},\ E_2v_{32}=E_3v_{23}. \qquad (5)$$

To make the calculation of the stress and strain in complex shape bodies made of orthotropic material easier, the constitutive relation for the isotropic material

$$\sigma_{ij}=2\mu\varepsilon_{ij}+\lambda\delta_{ij}\varepsilon_{kk}, \qquad (6)$$

is used, where δ_{ij} stands for Kronecker delta, and Lame's constants are given through the Young's modulus E and the Poisson's ratio v in the following relations

$$\lambda = \frac{vE}{(1+v)(1-2v)},\ \mu = G = \frac{E}{2(1+v)}. \qquad (7)$$

The Young's modulus and the Poisson's ratio for the orthotropic material, which is simulated by an isotropic material, are approximated by the least-square method (Heyden, 2000) as follows:

$$v = \frac{A_{11} + A_{22} + A_{33} + 4(A_{12} + A_{13} + A_{23}) - 2(A_{44} + A_{55} + A_{66})}{2[2(A_{11} + A_{22} + A_{33}) + 3(A_{12} + A_{13} + A_{23}) + (A_{44} + A_{55} + A_{66})]}$$

$$E = \frac{(1+v)(1-2v)}{15(1-v)}[3(A_{11} + A_{22} + A_{33}) + 2(A_{12} + A_{13} + A_{23}) + 4(A_{44} + A_{55} + A_{66})] \qquad (8)$$

where the coefficients A_{ij} are given by expressions (4).

Combining equations (1), (2) and (6), the following equations, expressed through unknown displacement, may be obtained:

$$\int_S \mu\left(\frac{\partial u_i}{\partial x_j} + \frac{\partial u_j}{\partial x_i}\right)n_j dS + \int_S \lambda\frac{\partial u_k}{\partial x_k}n_i dS + \int_V f_i dV = 0$$

$$(i=1,2,3) \qquad (9)$$

2.2 Boundary conditions
2.2. Granični uvjeti

In order to complete the mathematical model (9), the boundary conditions have to be specified. The surface traction f_{si} and/or the displacement u_s at the domain boundaries are known, i.e.

$$\sigma_{ij}n_j=f_{si} \qquad (10)$$

and/or

$$u_i=u_s. \qquad (11)$$
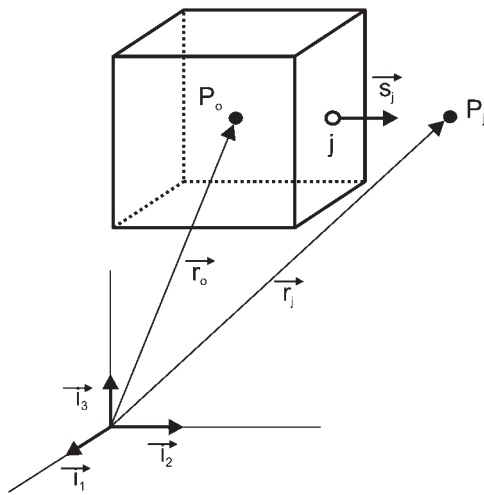
Figure 1 A typical control volume
Slika 1. Tipičan kontrolni obujam

3 NUMERICAL METHOD
3. NUMERIČKA METODA

The solution domain is discretized by a finite number of contiguous hexahedral control volumes (CV) or cells of the volume V which are bounded by six cell faces of the area S_j with calculation points P in the CV´s centres (Figure 1).

The equations of the mathematical model (9), expressed through unknown displacements, may be written for each control volume in the following form:

$$\sum_j \int_{S_j} \Gamma_{u_j} \frac{\partial u_j}{\partial x_j} dS_j + \int_V s_{u_i} dV = 0. \tag{12}$$

Coefficients Γ_{u_j} and s_{u_i} are given in Table 1.

The integrals in equation (12) are approximated by employing the midpoint rule, whereas the gradients are calculated by assuming the linear variation of dependent variables between the computational points. The result is a non-linear algebraic equation for each control volume of the following form (Demirdžić and Martinović, 1993):

$$a_{P_o} u_{iP_o} - \sum_{j=1}^n a_{P_j} u_{iP_j} = b_{u_i}, \tag{13}$$

where n stands for the number of internal faces of the observed control volume, and the coefficients are:

$$a_{P_j} = \Gamma_{u_j} \frac{S_j}{\delta x_j}, a_{P_o} = \sum_{j=1}^n a_{P_j}, b_{u_i} = s_{u_{iP_o}} V_{P_o} \tag{14}$$

where $s_{u_{iP_o}}$ is the value of the source term given in Table 1 at the central point P_O, and δx_j is the distance between the points, P_O and P_j.

After employing the boundary conditions, the sets of equations (13) for each displacement component are lineralized and temporarily "decoupled", so that the coefficients a and source term b are calculated by using the values of displacements from the previous iteration. In such a manner a system of linear algebraic equations is obtained, which is solved by an iterative procedure. More details can be found in (Demirdžić and Muzaferija 1995).

4 NUMERICAL ANALYSIS
4. NUMERIČKA ANALIZA

Two examples are considered in this chapter. The first one analyses the stress and strain in the corner joint, and the second in the chair skeleton construction. More examples may be found in (Hajdarević, 2006).

Certain assumptions were provided in numerical modelling of stress and strain:
- the material is isotropic and the elastic modulus and Poisson's ratio for the simulated materials are calculated by the method of least squares,
- joint is without glue line,
- force is acting on the final small area.

4.1 Example 1 − Corner joint
4.1. Primjer 1. Ugaoni spoj

In this section the corner mortise and tenon joint presented in Figure 2 are analyzed.

The material used for the corner joint is spruce, whose mechanic properties at temperature of 20ºC and with the moisture content of 9.8 % are given in Table 2,

Table 1 The meaning of Γ_{u_j} and s_{u_i} in equation (12)
Tablica 1. Značenje Γ_{u_j} i s_{u_i} u jednadžbi (12)

u_i	Γ_{u_1}	Γ_{u_2}	Γ_{u_3}	s_{u_i}
u_1	$2\mu+\lambda$	μ	μ	$\frac{\partial}{\partial x_j}\left(\mu\frac{\partial u_j}{\partial x_1}\right)+\frac{\partial}{\partial x_1}\left(\lambda\frac{\partial u_k}{\partial x_k}\right)-\frac{\partial}{\partial x_1}\left[(\mu+\lambda)\frac{\partial u_1}{\partial x_1}\right]+f_1$
u_2	μ	$2\mu+\lambda$	μ	$\frac{\partial}{\partial x_j}\left(\mu\frac{\partial u_j}{\partial x_2}\right)+\frac{\partial}{\partial x_2}\left(\lambda\frac{\partial u_k}{\partial x_k}\right)-\frac{\partial}{\partial x_2}\left[(\mu+\lambda)\frac{\partial u_2}{\partial x_2}\right]+f_2$
u_3	μ	μ	$2\mu+\lambda$	$\frac{\partial}{\partial x_j}\left(\mu\frac{\partial u_j}{\partial x_3}\right)+\frac{\partial}{\partial x_3}\left(\lambda\frac{\partial u_k}{\partial x_k}\right)-\frac{\partial}{\partial x_3}\left[(\mu+\lambda)\frac{\partial u_3}{\partial x_3}\right]+f_3$

Table 2 Mechanic properties of wood (spruce) (Bodig and Jayne, 1993)
Tablica 2. Mehanička svojstva drva (smrekovine) (Bodig and Jayne, 1993)

E_t	E_r	E_l	G_{rt}	G_{lr}	G_{lt}	ν_{tr}	ν_{rt}	ν_{rl}	ν_{lr}	ν_{tl}	ν_{lt}
GPa	GPa	GPa	GPa	GPa	GPa	-	-	-	-	-	-
0.392	0.686	15.916	0.0392	0.618	0.765	0.24	0.42	0.019	0.43	0.013	0.53

E – elastic modulus *(modul elastičnosti)*; *G* – shear modulus *(modul smicanja)*; *ν* – Poisson's ratio *(Poissonov koeficijent)*; *t* – tangential *(tangencijalni)*; *r* – radial *(radijalni)*; *l* – longitudinal *(longitudinalni)*

Figure 2 Corner mortise and tenon joint (left) and its dimensions (right)
Slika 2. Spoj sa skraćenim čepom: epruveta (lijevo), crtež (desno)

and according to (8) the corresponding Young's modulus is $E = 3.98$ GPa, while the Poisson's ratio is $\nu = 0.192$.

Because of the symmetry, one half of the joint is taken for the solution domain. Two elements are joined only by vertical side of tenon (face). Figure 3 presents the solution domain and the numerical grid.

The 30 000 CV grid is used for calculations, as it had been established that the results obtained with this grid may be considered grid-independent (Hajdarević 2006, Martinović *et al.* 2008).

The following boundary conditions are used to calculate the stresses and strains in the loaded corner joint:

- the fixed support of the lower corner joint end: zero displacements,
- the loaded end: force of 200N, acting at an angle of 45° was replaced by the uniform load on two perpendicular surfaces whose length equals the thickness of the corner joint, and whose width equals the width of CV,
- other exterior surfaces: stress free,

- the clearance in the zone of joint (0.6 mm and 3 mm): the conditions taken are the same as for the free surface, i.e. the corresponding stress components equal zero.

The displacement field of the corner joint and the deformed joint are shown in Figure 4. The maximum displacement of 0.66 mm is at the free end of the joint.

The field of normal stresses σ_{xx} and σ_{yy} and the shear stresses τ_{xy} and τ_{xz} are shown in Figure 5.

The maximum compressive stresses ($\sigma_{xx} = -9.3$ MPa and $\sigma_{yy} = -6.6$ MPa) occur on the inner surface of the corner joint, and the maximum tensile stress ($\sigma_{xx} = 6.6$ MPa and $\sigma_{yy} = 2.2$ MPa) on the outer surfaces. These values are smaller than the allowable compressive stress parallel to the grain of 11 MPa, i.e. the tensile stress of 10.5 MPa (Kollmann and Côté, 1968).

The extreme values of the shear stresses are $\tau_{xy} = 2.28$ MPa and $\tau_{xz} = 2.43$ MPa. It is extremely important for the corner joints that the shear stress is within the allowable values. Bearing that in mind, Figure 6 shows the distribution of the total shear stress on the reduced
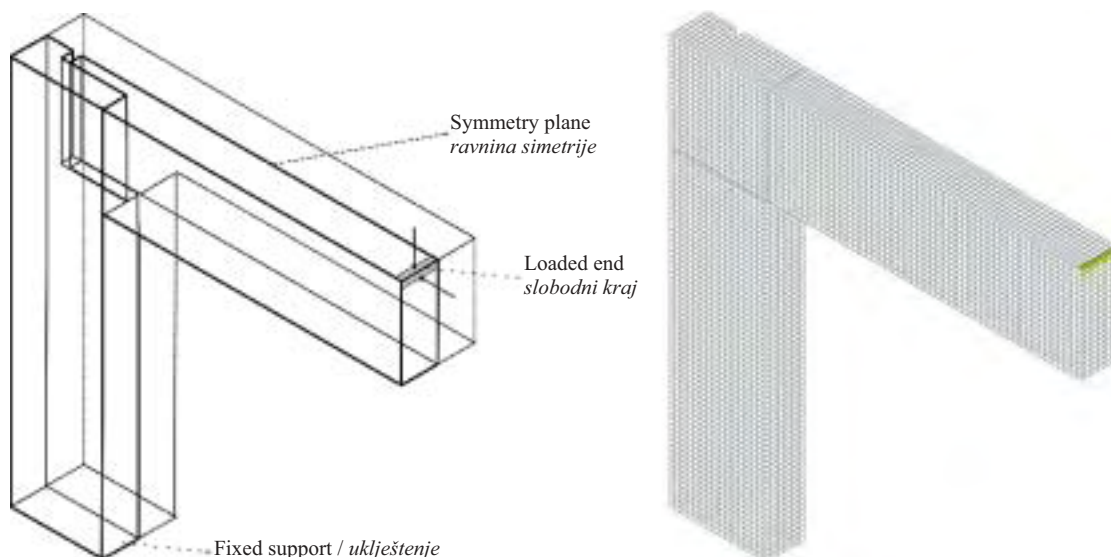
Figure 3 Corner joint: solution domain and boundary conditions (left), numerical grid (right)
Slika 3. Kutni spoj: područje rješavanja i rubni uvjeti (lijevo), numerička mreža (desno)
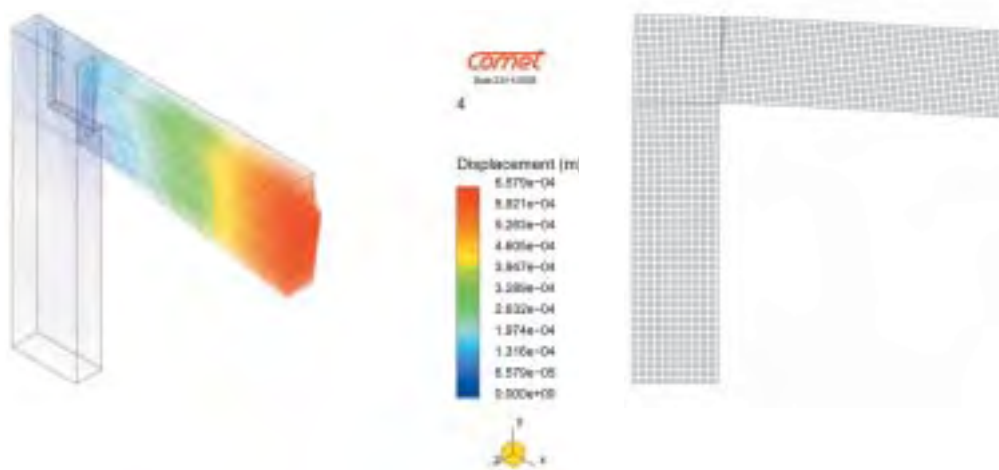
Figure 4 Total displacement field (left), deformed joint (right)
Slika 4. Područje ukupnog pomaka (lijevo), deformirani kutnik (desno)
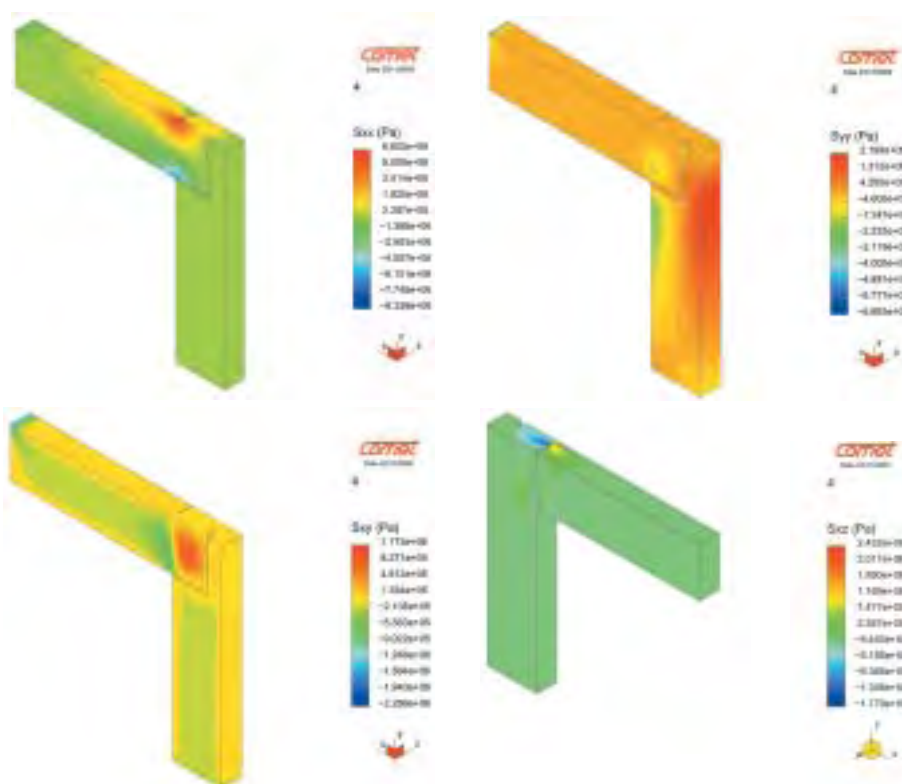
Figure 5 Distribution of normal stresses σ_{xx} and σ_{yy} (above) and of shear stresses τ_{xy} and τ_{xz} (below)
Slika 5. Raspodjela normalnih naprezanja σ_{xx} i σ_{yy} (gore) i raspodjela posmičnih naprezanja τ_{xy} i τ_{xz} (dolje)
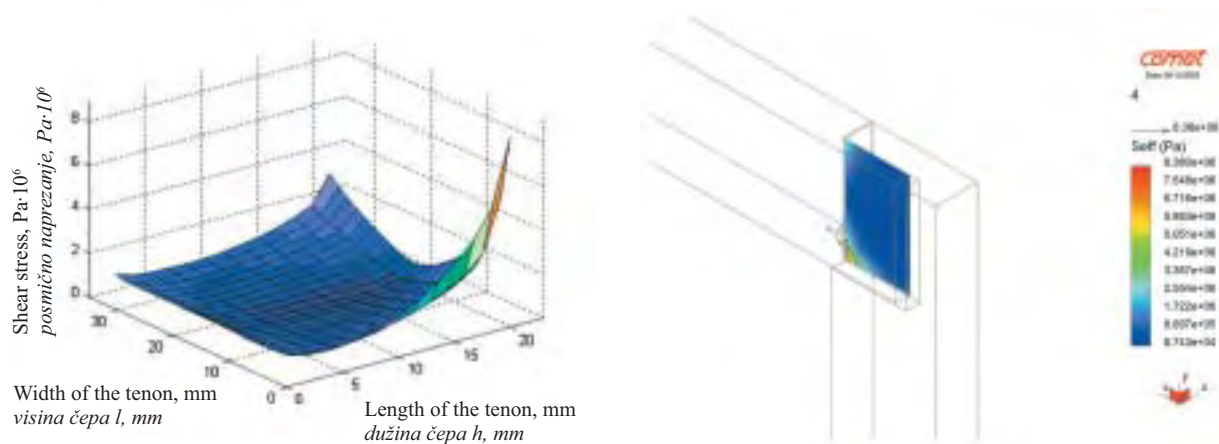
Figure 6 Distribution of shear stress on the contact surface of joint parts
Slika 6. Raspodjela ukupnoga posmičnog naprezanja na kontaktnoj površini dijelova spoja
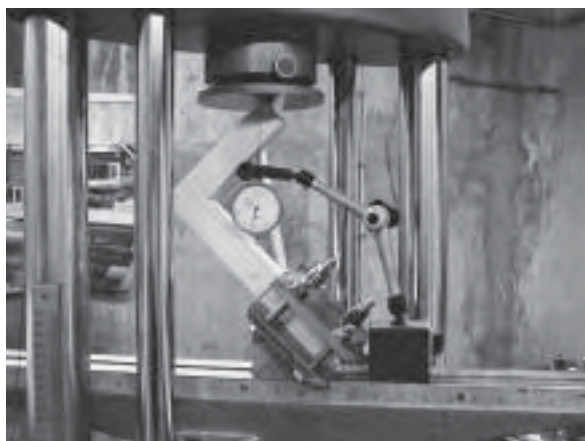
Figure 7 Laboratory measurement of the joint edge point displacement
Slika 7. Laboratorijsko određivanje pomaka rubne točke kutnika
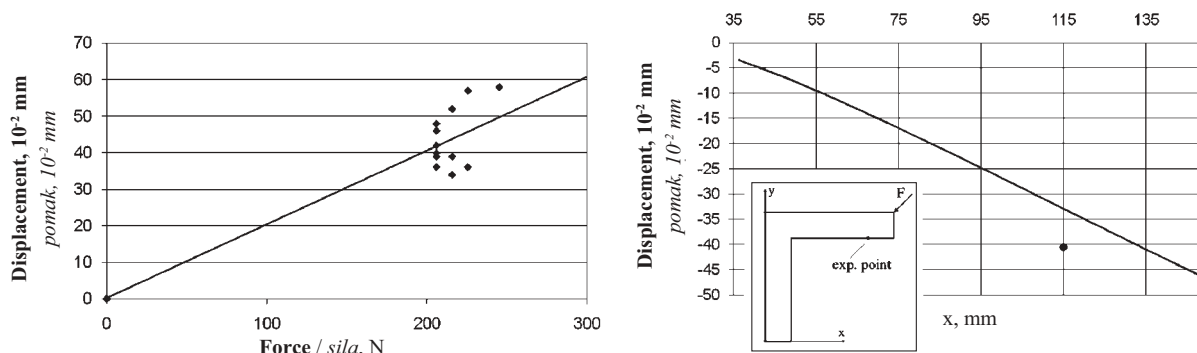
Figure 8 Experimentally determined displacement in the reference point (left) and distribution of displacement along the directions parallel to that of the load action at the intersection of planes $y = 115.8$ mm and $z = 13.2$ mm for the corner joint and the experimentally obtained displacement (right)
Slika 8. Eksperimentalno određen pomak u referentnoj točki (lijevo) i raspodjela pomaka duž pravaca paralelnih s pravcem djelovanja opterećenja u presjeku ravnina $y = 115.8$ mm i $z = 13.2$ mm za kutni spoj i eksperimentalno dobiven pomak (desno)

tenon, i.e. on the contact surface of the parts of the corner joint, which is at the distance of $z = 4.6$ mm from the symmetry plane.

The maximum value of the shear stress is 8.3 MPa and it occurs at around 0.36% of the contact surface of the joint parts. Given that the shear strength parallel to the grain ranges between 4 and 20 MPa (Kollmann and Côté, 1968), the corner joint will support the applied load.

To verify the calculation results, the displacement of the edge point of the joint in the direction of the force action is measured, as shown in Figure 7.

The total of 15 corner joints, whose shape and dimensions are equal to those shown in Figure 2, were examined. The resulting dependence of the load of the joint edge point displacement is shown in Figure 8 (a). Figure 8 (b) shows the numerically obtained distribution of the displacement along the directions parallel to the direction of the load action at the intersection of planes $y = 115.8$ mm and $z = 13.2$ mm. Figure 8 also shows the displacement obtained experimentally, which is greater than the calculated one for about 18%.

4.2 Example 2 − Skeleton chair construction
4.2. Primjer 2. Okvirna konstrukcija stolice

Due to symmetry only a half of the chair presented in Figure 9 is analyzed. The dimensions of cross section of elements are 24x40 mm (p_1) and 16x24 mm

(p_2). Tenon dimensions of the side rail and the back leg joint are: thickness 8mm, length 16 mm and width 40 mm. Chair elements are joined only by face of tenon. There are clearances (2 mm) between all other contact surfaces. The mass load of the horizontal lower skeleton of the entire chair is 100 kg. The vertical frame mass load is 22 kg. The others surfaces are unloaded. The chair is assumed to be fixed to the ground, i.e. the displacement in those points equals zero. The chair material is spruce, having the same properties as in the previous example. The calculation was done on the grid of 24329 CV (Figure 9).

The distribution of the dominant normal stress σ_{yy} on the chair skeleton surface and joints is shown in Figure 10. The maximum value of this stress is 10.7 MPa, both in the tensile and the compression zone and it occurs in the joint of the side rail and the back leg.

The maximum values of the shear stress occurs at the same place. The distribution of the stresses σ_{xz} and σ_{xy} and the total shear stress on the tenon surface i.e. in the surface $x = 0.202$ m is shown in Figure 11.

The maximum shear stress values $\tau_{xz} = 6$ MPa and $\tau_{xy} = 5.6$ MPa and the value of total shear stress in that plane ($x = 0.202$ m) is about 8.2 MPa. The maximum shear stress occurs at about 2.5% of the total contact surface. The maximum values of both the normal and the shear stresses are within the allowable values (Kollmann and Côté, 1968).
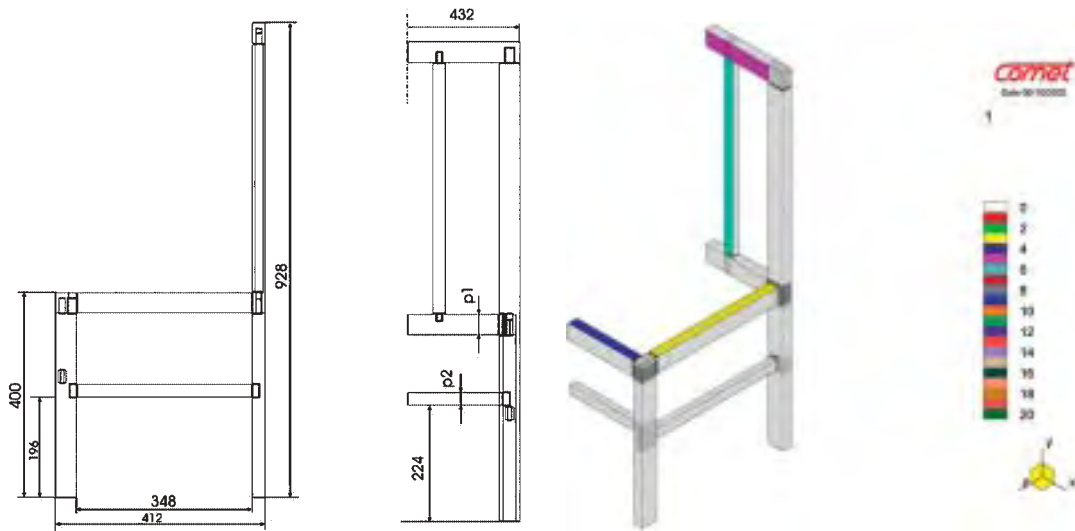
Figure 9 Chair skeleton construction (left), solution domain and numerical network (right)
Slika 9. Okvirna konstrukcija stolice (lijevo), područje rješavanja i numerička mreža (desno)
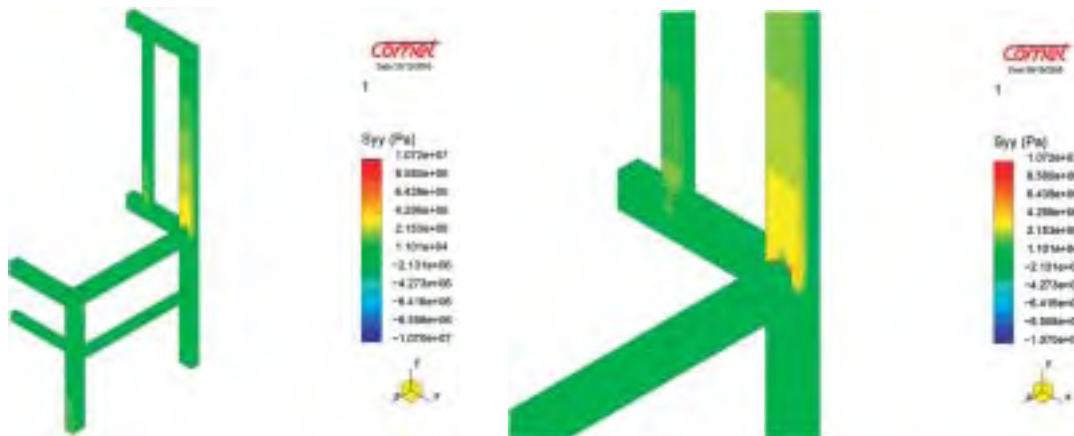
Figure 10 Distribution of stress σ_{yy} on the chair contour (left), and in the joint zone (right)
Slika 10. Raspodjela normalnog naprezanja σ_{yy} na nožištu stolice (lijevo) i u zoni spoja (desno)
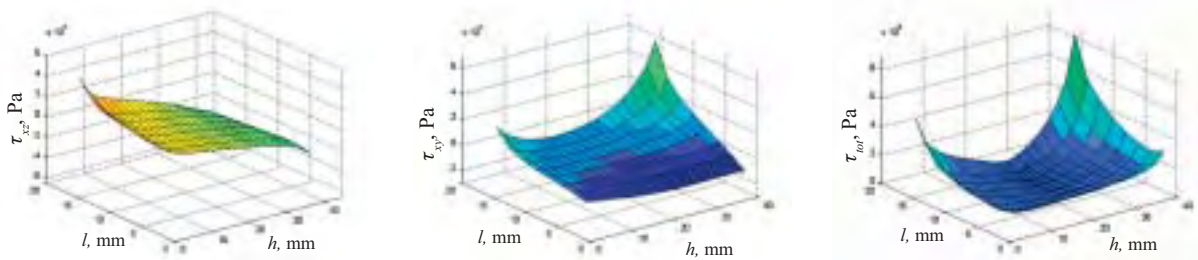
Figure 11 Distribution of shear stress in the contact pointing at the joint between the side rail and the back leg τ_{xz} (left), τ_{xy} (middle) and total shear stress τ_{tot} (right) (l – length of the tenon, mm; h – width of the tenon, mm)
Slika 11. Raspodjela posmičnog naprezanja u kontaktnoj površini spoja bočnog poveznika i stražnje noge, τ_{xz} (lijevo), τ_{xy} (u sredini), ukupno posmično naprezanje τ_{tot} (desno) (l – dužina čepa, mm; h – visina čepa, mm)

The chair deformation is shown in Figure 12. The largest displacement of around 13 mm occurs at the far end points of the chair back. That is an unusually large displacement, because the calculations are done for the chair made of soft wood, the material used in Example 1.

5 CONCLUSION
5. ZAKLJUČAK

This paper presents, for the first time, the development and the application of the finite volume method for predicting the distribution of displacements and stresses in the wooden corner joints and chair skeleton construction.

The numerical stimulation of stresses in a complex chair skeleton construction has shown that the construction strength depends on the stress values in the corner joints, primarily in the joint connecting the side rail and the chair back leg where both the maximum normal and shear stresses occur. Stiffness analysis has shown that the greatest deformation occurs in the points of the free end of the back of the chair. Thus,
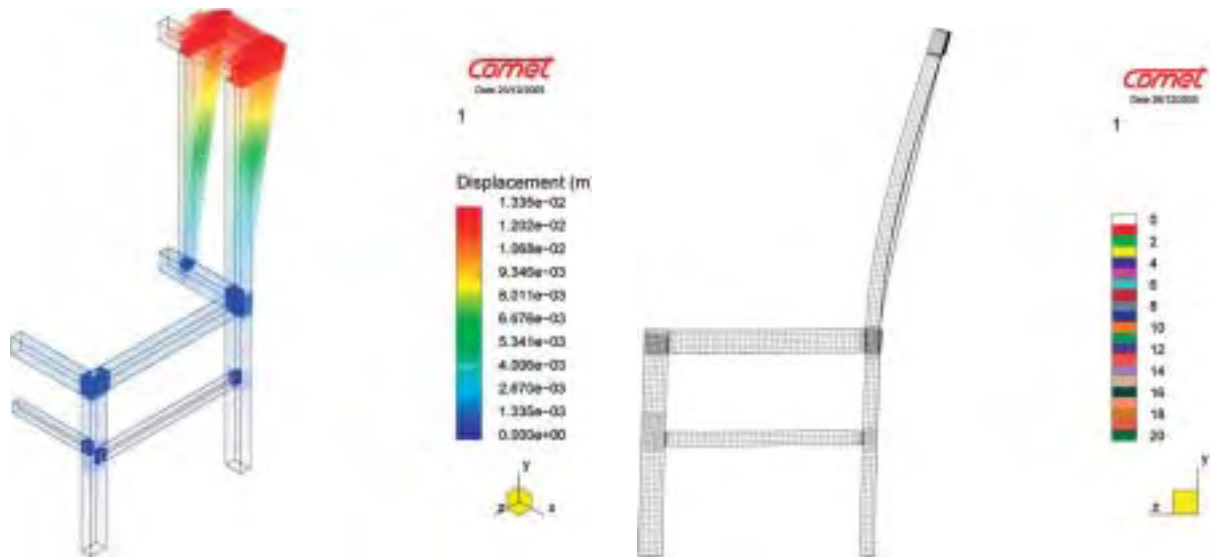
Figure 12 Distribution of the total displacement (left) and (right) the strained skeleton chair (10× increase)
Slika 12. Raspodjela ukupnog pomaka (lijevo) i deformirani okvir stolice (uvećanje10 puta, desno)

the mathematical model and the numerical calculation employing the finite volume method presented enable the design and the construction of a chair.

6 REFERENCES
6. LITERATURA

1. Bodig, J.; Jayne, B. A. 1993: Mechanics of Wood and Wood Composites, Krieger Publ. Comp. Malabar, Florida.
2. Demirdžić, I.; Horman, I.; Martinović, D. 2000: Finite volume analysis of stress and deformation in hygro-thermo-elastic orthotropic body, Comput. Methods Appl. Mech. Engrg., 190: 1221-1232.
3. Demirdžić, I.; Martinović, D. 1993: Finite volume method for thermo-elasto-plastic stress analysis, Comput. Methods Appl. Mech. Engrg., 109: 331-349.
4. Demirdžić, I.; Muzaferija, S. 1995: Numerical method for coupled fluid flow, heat transfer and stress analysis using unstructured moving meshes with cells of arbitrary topology, Comput. Methods Appl. Engrg., 125:235-255.
5. Hajdarević, S. 2006: Strength analysis of joints in wooden constructions, MSc Thesis (in Bosnian), University of Sarajevo, Mechanical Engineering Faculty, Sarajevo.
6. Heyden, S. 2000: Network Modelling for the Evaluation of Mechanical Properties of Cellulose Fibre Fluff, Doctoral thesis, Lund University, Department of Mechanics and Materials, Lund, Sweden.
7. Horman I., Martinović D.; Hajdarević S. 2008: Numerical Analysis of a Phenomena in the Wood caused by Heat, Moisture or External Laod, International scientific conference: Challanges in forestry and wood technology in the 21th century, University of Zagreb, Faculty of Foresty, Zageb, Proceedings pp. 31-34.
8. Horman, I., Martinović, D.; Hajdarević, S. 2009: Finite Volume Method for Analysis of Stress and Strain in Wood, Drvna industrija, 60 (1): 27-32.
9. ICCM-Institute of Computational Continuum Mechanics GmbH 2001: User Manual – Comet version 2.00, Hamburg.
10. Kollmann, F. P.; Côté, W. A. 1968: Principles of Wood Science and Technology, Springer – Verlag, New York, 592 p.
11. Martinović, D.; Horman, I.; Demirdžić, I. 2001: Numerical and Experimental Analysis of a Wood Drying Process, Wood Science and Technology, 35: 143-156.
12. Martinović, D.; Horman, I.; Hajdarević, S. 2008: Stress Distribution in Wooden Corner Joints, Strojarstvo 50 (4): 193-204.
13. Nicholls, T.; Crisan, R. 2002: Study of the stress-strain state in corner joints and box-type furniture using Finite element analysis, Holz als Roh- und Werkstoff, 60: 66-71.
14. Olsson, P.; Olsson, K. G. 2003: Applied visualization of structural behaviour in furniture design, Chalmers University of Technology, Geteborg, Sweden.
15. Pousette, A. 2003: Full-scale test and finite element analysis of a wooden spiral staircase, Holz als Roh- und Werkstoff, 61: 1-7.
16. Pousette. A. 2006: Testing and modeling of the behavier of wooden stairs and stair joint, J. Wood Science, 52: 358-362.
17. Slattery, J. C. 1981: Momentum, Energy and Mass Transfer in Continua, Kriger Publishing Company, Huntington, New York.
18. Smardzewski, J.; Papuga, T. 2004: Stress Distribution in Angle Joints of Skeleton Furniture, Electronic Journal of Polish Agricultural Universities, Wood Technology 7 (1).
19. Smardzewski, J.; Prekrat, S. 2002: Stress Distribution in Disconnected Furniture Joints, Electronic Journal of Polish Agricultural Universities, Wood Technology 5 (2).

Corresponding address:

Associated professor IZET HORMAN, Ph.D.

Faculty of Engineering
University of Sarajevo
Vilsonovo šetalište 9
71000 Sarajevo
Bosnia and Herzegovina
e-mail: horman@mef.unsa.ba